PERGAMON

Journal of Structural Geology 25 (2003) 923–934

JOURNAL OF STRUCTURAL GEOLOGY

www.elsevier.com/locate/jsg

Preferred orientation of planar microstructures determined via statistical best-fit of measured intersection-lines: the 'FitPitch' computer program

Domingo Aerden*

Departamento de Geodinamica, Universidad de Granada, Granada 18071, Spain

Received 30 July 2001; received in revised form 10 July 2002; accepted 15 July 2002

Abstract

The 'FitPitch' computer program allows characterisation of preferred orientation of planar microstructures in a rock from the orientations of their intersection-lines on different sections. Measured pitch or strike angles of such intersection-lines are fitted to the theoretical intersection-lines of a single model-plane, or a combination of two or three model-planes. The degree of fit is quantified in terms of the deviation between natural and theoretical intersection-lines, normalised by uniform data. A first application is described concerning porphyroblast inclusion trails whose orientation in 28 samples from the Variscan Iberian Massif was measured. Analysis of these data illustrates how the method can be used to quantify preferred orientation of relict foliations contained in a group of porphyroblasts and how this complements existing techniques for determining foliation intersection axes (FIA) in porphyroblasts. A second described application deals with previously published orientation data for microfracture trace lines in quartz grains of a Variscan granite in the Rhine Graben. Qualitatively established best-fit planes derived originally from this data are compared with the numerically established planes using the FitPitch program, and discussed in terms of the advantages and potential limitations of the method.

Keywords: Microstructural analysis; Preferred orientation; Porphyroblast; Inclusion trails; Microfracture

1. Introduction

The use of porphyroblast inclusion trails as kinematic indicators faces the difficulty that these microstructures represent planar (2-D) cuts through often complex and potentially variable microstructures in a rock. Consequently, considerable efforts have been undertaken to complement traditional qualitative study of selected porphyroblasts in 2-D with new quantitative approaches concerned with 3-D data for large porphyroblast populations (Johnson, 1990; Hayward, 1992; Davis, 1993; Huang, 1993; Aerden, 1994, 1995, 1998; Guglielmo, 1994; Bell et al., 1995, 1997, 1998; Mares, 1998; Bell and Mares, 1999; Jung et al., 1999; Ilg and Karlstrom, 2000). Confirming an early report (Fyson, 1980), these studies have revealed well developed preferred orientation of planar and linear porphyroblast microstructures in different metamorphic belts, commonly contrasting with much more variable orientation of dominant matrix fabrics. It has been shown further how such information can be applied to correlate complex (polyphase) deformation histories, and how 2D inclusion trail geometries alone can lead to incomplete or erroneous kinematic interpretations (e.g. Aerden, 1994).

As a methodological contribution to the above-mentioned new line of research, a computer program has been developed that allows quantitative characterisation of the spatial preferred orientation of foliation relicts preserved in porphyroblasts. This is done by fitting inclusion trail orientations measured from differently oriented thin-sections to one, two or three best-fit planes in order to characterise potential unimodal, bimodal or trimodal preferred orientation patterns. The program can be applied equally to analyse other planar microstructures which may occur as one or multiple orientational sets, such as microfractures as will be shown further.

After a brief review of current 3-D microstructural techniques and a description of program principles, the results of two applications are presented and discussed. The first application concerns porphyroblastic samples from the Variscan orogen in NW-Iberia, and illustrates various advantages and limitations of the method as compared

* Tel.: +349-5827-2883; fax: +349-5824-8527.
E-mail address: aerden@ugr.es (D. Aerden).

0191-8141/03/$ - see front matter © 2002 Published by Elsevier Science Ltd.
PII: S0191-8141(02)00119-0

with previous 3-D techniques. A forthcoming paper in this journal (Aerden, 2002) will address the relationship of these results with field structures in NW-Iberia and tectonic implications.

The second application described in this paper concerns previously published microfracture orientation data from four granite samples (Dezayes et al., 2000). The original workers measured microfracture trace lines (fluid-inclusion trails) in quartz grains and fitted their data 'manually' to multiple best-fit planes. A comparison of their results with the best-fit solutions obtained via FitPitch reveals interesting coincidences and some differences.

2. Previous 3-D microstructural methods

2.1. Qualitative fitting of data using a stereonet

The spatial preferred orientation of foliation relicts in porphyroblasts (i.e. inclusion planes) can be determined simply if inclusion trails show well developed unimodal orientation maxima for differently oriented thin-sections. These modal maxima can be plotted as points on a stereonet and fitted to a great circle (Jung et al., 1999). However, complications arise when inclusion trails show bimodal, trimodal or relatively scattered orientations in a thin-section, potentially corresponding to multiple foliation generations. Fitting such data requires previous correlation of different 2-D maxima between different thin-sections, which can be ambiguous. The FitPitch program eliminates the need to interpret or correlate multimodal 2-D maxima by fitting data individually.

2.2. The FIA method

Hayward (1990) developed a technique to determine the spatial orientation of foliation-intersection axes (i.e. crenulation axes) or foliation-inflexion axes (i.e. axes of relative matrix-porphyroblast rotation) from asymmetrically crenulated or curved inclusion trails (e.g. sigmoidal, spiral or staircase geometry). Such microstructures (generally abbreviated as FIA) can be measured by recording the predominant curvature asymmetry of inclusion trails ('S' or 'Z') in sets of vertical thin-sections with different strikes around the compass. This allows the trend of a FIA to be constrained between the strikes of two adjacent thin-sections (of the radial set) that mark a switch in dominant curvature asymmetry. The FIA plunge can be subsequently determined in a similar way by cutting additional thin-sections radially about a horizontal axes oriented perpendicular to the FIA trend. Bell et al. (1995) refined the method to allow determination of multiple FIA in rocks with complex structural evolution from consistent curvature-sense reversals of inclusion trails as they pass from the core to the rim of individual porphyroblasts. The usefulness of FIA data for unravelling orogenic histories, or studying fundamental deformation processes at various scales has been convincingly demonstrated since then (e.g. Bell et al., 1998; Mares, 1998; Bell and Mares, 1999; Hickey and Bell, 1999; Stallard and Hickey, 2001; Aerden, 2002). However, in the author's experience, porphyroblastic rocks are commonly unsuitable for the FIA method, because they contain mainly straight inclusion trails, inclusion trails showing inconsistent curvature senses in the same thin-section (while lacking the earlier mentioned core-rime relationships), or symmetrically crenulated inclusion trails. Via calculation of multiple best-fit planes, FitPitch can still furnish best-fit FIA for such samples.

2.3. 3-D imaging of single porphyroblasts

The internal geometry of individual large porphyroblasts can be resolved in great detail by combining 2-D images of a series of closely spaced thin-sections in a 3-D reconstruction using various image-analysis techniques (Schoneveld, 1979; Johnson, 1993; Johnson and Moore, 1996; Jung et al., 1999). Another promising imaging technique recently applied to metamorphic textures (after earlier use in the medical- and materials sciences) is high-resolution computed X-ray tomography (Denison et al., 1997). Such techniques represent valuable tools for fundamental studies of the processes involved in synkinematic porphyroblast growth, and for detailed reconstruction of $P–T–t$ trajectories. However, they are less suitable for the analysis of a large number of porphyroblasts as required in regional tectonic studies.

3. Program principles

3.1. Fitting intersection-lines

The program is written in FORTRAN and fits inclusion-trail orientations (i.e. pitch angles or strike angles for horizontal sections) gathered from differently oriented thin-sections to one, two or three planes. Inclusion trails are treated as intersection-lines of one or several foliation planes (i.e. inclusion planes) on different thin-section planes. Therefore, data are compared with the intersection-lines of a large number of uniformly spaced model-planes on the same sections. A best model-plane or a best combination of two or three model-planes can be identified by minimising the deviation between data (i.e. natural intersection-lines) and model intersection-lines. This is fundamentally different from fitting lines that do not represent the intersection of two planes (e.g. bedding poles), which is done by minimising their angular deviation from the planes themselves (Ramsay, 1967; Aerden and Sanchez San Roman, 2002).

The difficulty of fitting data to multiple planes resides in the huge number of combinations that can be formed with only a limited number of elements. For a resolution of 1° in

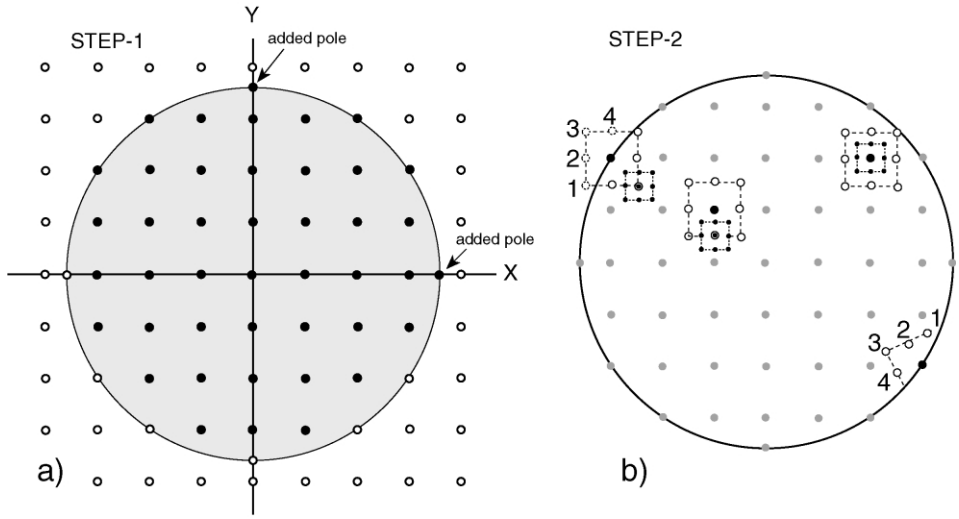

Fig. 1. (a) Forty-three model-planes tested during STEP-1 obtained by superposing a rectangular grid on an equal-area stereonet and adding two poles on the plot circle. (b) Hypothetical test-pole definition during the first two iterations of STEP-2 about the poles of the preliminary best planes obtained from STEP-1 (the larger black dots). Poles that fall outside the primitive circle (numbered 1–4) are transferred to the opposite side of the stereonet.

spherical coordinates, 32401 planes can be defined with which one can form 5.1×10^8 different combinations of two planes, and over 5.4×10^{12} combinations of three planes. Testing all of them is not practical even with modern computers. Therefore, the strategy is adopted of first (STEP-1) considering a reduced set of coarsely-spaced model-planes, and then (STEP-2) iteratively refining a preliminary solution obtained with this set.

3.2. STEP-1: calculation of a preliminary best-fit solution

The initial group of coarsely spaced model-planes is defined by superposing a square grid on an equal-area stereonet and taking grid-line intersections as the poles of model-planes. Two additional poles are added on the primitive circle to fill remaining gaps so that a total of 43 model poles is obtained (Fig. 1a). After the user has specified if he desires to fit data to one, two or three planes, the program calculates the pitches of all intersection-lines of the 43 planes on the thin-sections. These 'model pitches' are stored in a two-dimensional matrix called MODEL-PITCH(i,j), where 'i' identifies a model-plane and 'j' a thin-section. From this point onward, the program follows different, but analogous paths for one-, two- or three-plane fitting. The remainder of this section will only consider the case of a three-plane fit.

For three-plane fitting, the heart of the program is an algorithm containing four nested loops ('do' statements in FORTRAN; see Appendix A) that test all possible plane triplets (12341 total) that can be formed with the initial 43 planes. Each plane triplet is tested as follows. The angular deviations of the first datum from three model intersection-lines on that section are determined. The smallest deviation is stored in memory and the datum is attributed to the corresponding model-plane (i.e. producing the nearest intersection-line). The deviations of the datum from the other two intersection-lines are further ignored. The same is repeated for the second datum, the third, and so on until the last datum from the last thin-section. The sum of all smallest deviations (i.e. 'total deviation') is stored in a 3-D array called SCORE(i,j,k), where i, j and k identify the tested model-plane triplet. After the above has been repeated 12341 times for all plane triplets, the smallest value in SCORE(i,j,k) is searched and the corresponding plane triplet (i,j,k) identified as the (preliminary) best-fit solution.

3.3. STEP-2: iterative refinement

To refine the preliminary solution (STEP-1), the original grid spacing is first reduced by half and a new set of 27 test poles is defined, distributed in three square clusters about the poles of the preliminary best planes (Fig. 1b). Poles falling outside the plot circle are automatically transferred to the opposite side of the stereonet. New model-plane triplets are then formed by taking one pole out of each cluster giving a total of 729 ($=9^3$) new plane triplets. All these are tested identically as described for STEP-1. The newly obtained best-plane triplet is returned to the start of STEP-2 to perform a new iteration, which commences with again halving the previously used grid spacing and redefining 27 model poles at smaller distances about the last best poles. After four iterations (not counting STEP-1) a resolution of approximately 1° is reached and the definitive best-fit planes are determined. These are printed with the corresponding FIA (intersection-lines of best-fit planes), average and standard deviations of data from model intersection-lines, and three groups of data as fitted to three planes.

Table 1
Quantitative FitPitch results for three porphyroblastic samples from NW-Iberia plus four granite samples of Dezayes et al. (2000). Data sets are called after sample numbers with the suffixes 'A' and 'B' referring to A-type or B-type inclusion-trails (see text). α_d is the average angular deviation between measured and model intersection-lines. α_m is the average deviation between best-fit lines calculated for separate thin-sections, and best-fit intersection-lines based on all data. R_d and R_d are the corresponding values normalised by uniform data. The selection of one of three possible solutions (bold numbers) is based on the highest R_d and R_m values

	No. of model planes	α_d	α_m	R_d	R_m	Poles of best-fit planes (azimuth/plunge)
RESULTS FOR PORPHYROBLAST DATA						
Data: 3 + 4B	1	34.8	32.3	1.29	1.40	117/65
$N = 118$	**2**	16.6	7.1	1.43	3.31	173/69; 099/06
Sections: 7	3	11.8	9.7	1.53	2.25	117/48; 131/02; 270/79
Data: 21A	1	14.6	11.9	3.07	3.79	072/05
$N = 52$	2	7.9	10.6	3.95	2.94	271/16; 068/09
Sections: 3	**3**	4.7	2.7	5.58	9.74	271/07; 072/12; 241/16
Data: 27A + B	1	38.1	35.6	1.27	1.27	166/15
$N = 195$	2	21.3	17.7	1.14	1.37	156/10; 045/88
Sections: 7	**3**	13.6	9.2	1.38	2.05	167/17; 235/48; 315/20
RESULTS FOR MICROFRACTURE DATA						
Data: I	1	37.9	37.9	1.19	1.19	259/28
$N = 1098$	**2**	16.9	5.1	1.51	4.98	172/06; 081/34
Sections: 3	3	12.2	9.5	1.41	1.80	177/42; 258/10; 128/13
Data: II	1	37.9	37.1	1.19	1.13	283/12
$N = 1622$	**2**	16.9	2.1	1.37	10.80	295/02; 035/68
Sections: 3	3	12.6	10.1	1.30	1.62	185/19; 294/03; 048/56
Data: III	1	33.6	33.1	1.34	1.36	000/00
$N = 1119$	2	16.8	4.5	1.46	5.44	175/07; 303/47
Sections: 3	**3**	11.4	3.2	1.47	5.23	328/01; 217/25; 096/29
Data: IV	1	35.6	35.5	1.26	1.27	216/30
$N = 810$	**2**	18.1	6.7	1.36	3.67	182/20; 084/47
Sections: 3	3	12.0	6.6	1.32	2.42	215/42; 002/44; 093/04

3.4. STEP-3: evaluation of results

The degree of fit is expressed in terms of the average angular deviation between data and the model intersection-lines (α_d), normalised by uniform data. The latter is necessary, because uniform data will, generally, yield a smaller average deviation for any combination of three model-planes than two or one model-planes. Thus, the deviations of all data from their nearest model intersection-lines are summed and divided by the total number of data to obtain α_d. Then, the same is done for uniform data, and the ratio $R_d = \alpha_u/\alpha_d$ is calculated as a measure of the quality or 'tightness' of a best-fit solution (α_u is the average deviation of uniform data from the model intersection-lines). The probability that randomly generated data yield a particular R_d value is $P_1 = 1/(R_d^{N-2})$, $P_2 = 1/(R_d^{N-4})$, or $P_3 = 1/(R_d^{N-6})$ for one-, two- or three-plane fitting, respectively, N being the number of data. The differences between these expressions stem from the fact that the first six, four or two data can always be perfectly fitted to three-, two-, or one planes, respectively. However, if N is relatively large, R_d for one-, two- and three-plane fits can be compared to choose the statistically more significant solution. For example, the microfracture data for sample I of Dezayes et al. (2000) (Table 1) yield average deviations of 16.9 and 12.2° in two- and three-plane solutions, respectively, yet the former is statistically favoured ($R_d = 1.51$ versus $R_d = 1.41$).

An additional criterion on which the choice of a particular solution can be based is the degree to which a best-fit solution is consistent with the orientation of (2-D) modal maxima of separate thin-sections. To quantify this, one, two or three best-fit lines are calculated for the data of individual thin-sections separately. The average deviation (α_m) of these lines from the best-fit intersection-lines as based on all sections, normalised by uniform data, yields the ratio $R_m = \alpha_u/\alpha_m$ which measures the degree of internal consistency of a data set.

3.5. Other user-specified fit parameters

Besides specifying whether a best-fit with one, two or three planes is desired, an additional parameter must be entered by the user related to the fact that inclusion planes subparallel to a thin-section are unlikely to produce a visible inclusion trail line on it. Thus, a minimum cut-angle between thin-sections and inclusion planes must be defined below which an inclusion trail line is no longer attributable to that plane. Estimating this angle is somewhat arbitrary

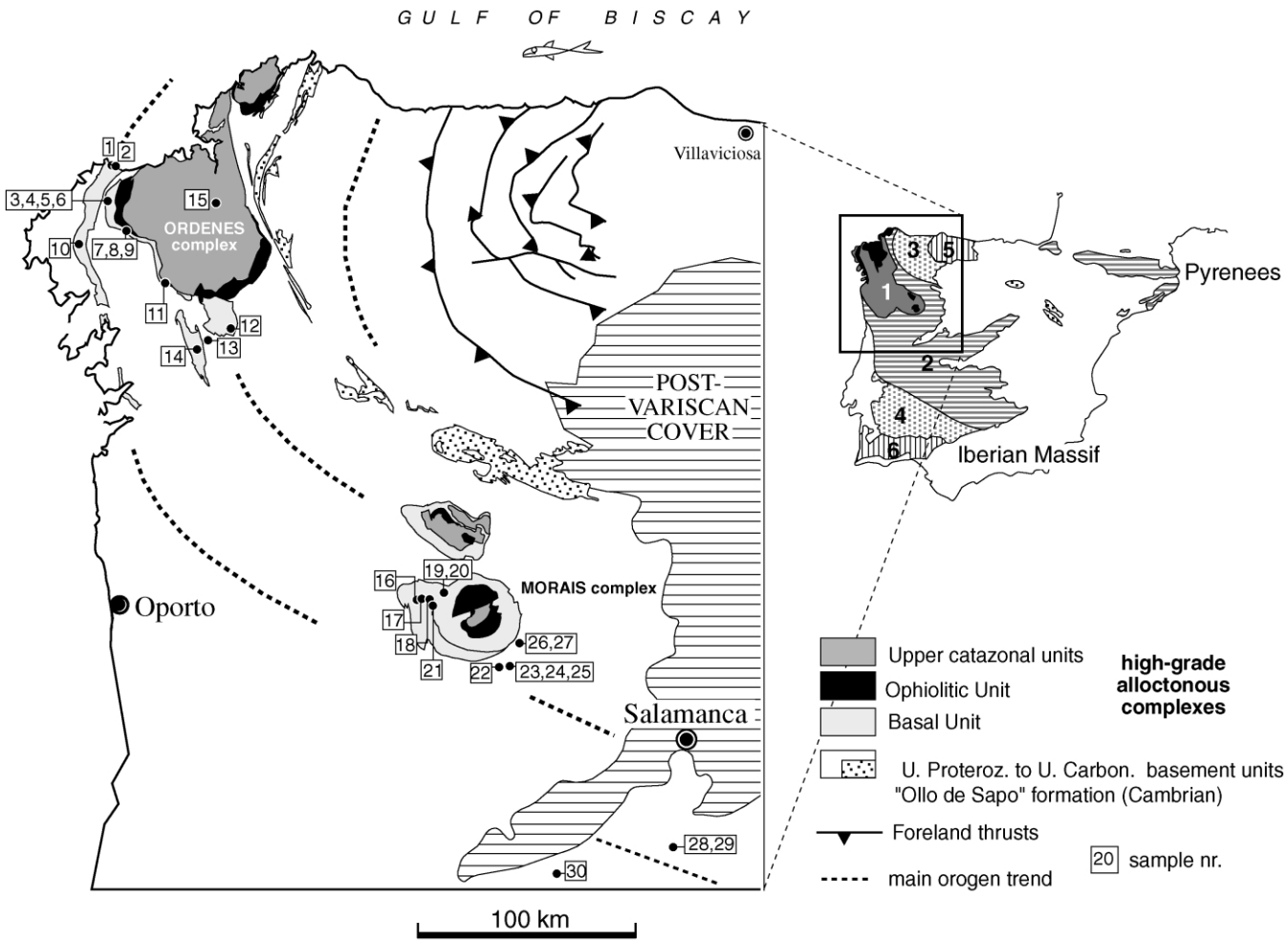

Fig. 2. Simplified map of NW-Iberia showing the location of analysed porphyroblastic samples from the Variscan Iberian Massif. 1: Galicia-Tras-os-Montes Zone (para-autochthonous) carrying several high-grade allochthonous klippen (solid black). 2: Central-Iberian Zone. 3: West-Asturian-Leonese Zone. 4: Ossa-Morena Zone. 5: Cantabrian Zone. 6: South-Portuguese Zone.

and depends on the coarseness, spacing, definition etc. of inclusion trails, and on the type of microstructure that is being analysed. For the porphyroblastic samples considered in this paper, minimum cut angles were estimated as 5 and 10° for A- and B-type microstructures (see further), respectively. For the microfracture data the angle was taken as 10°. However, slightly different values did not appear to have a significant effect on the final results. Finally, the user can choose between giving equal weight to individual porphyroblast measurements, as in the present study, or attribute equal weight to individual thin-sections regardless of the number of data supplied by each.

4. Fitting inclusion-trail orientations in NW-Iberia

4.1. Geological setting

The Iberian Massif is a segment of the European Variscan orogen built during the Devono-Carboniferous Gondwana–Laurentia collision. An allochthonous nappe complex composed of Lower Palaeozoic metasediments, orthogneisses, granulites and eclogites is discontinuously exposed in several synclinal massifs or tectonic klippen (Ries and Shackleton, 1971; Fig. 2). These are carried by a more continuously exposed para-autochthonous nappe comprising mainly Silurian slates and schists. The larger part of the Iberian Massif, however, comprises the footwall of the above-mentioned nappes, and is traditionally subdivided into five zones with contrasting structural styles and palaeogeographic significance (Fig. 2). The Central Iberian Zone (CIZ) forms the backbone of the orogen with high- to medium-grade Upper-Proterozoic and Palaeozoic rocks intruded by abundant syn- and post-orogenic granitoids. This zone is characterised by large upright folds overprinted by younger flat-lying foliations and detachments. The West-Asturian-Leonese Zone (WALZ) and Ossa-Morena Zone (OMZ) occupy intermediate positions in the orogen on both sides of the CIZ. They exhibit large recumbent fold-nappes moderately refolded

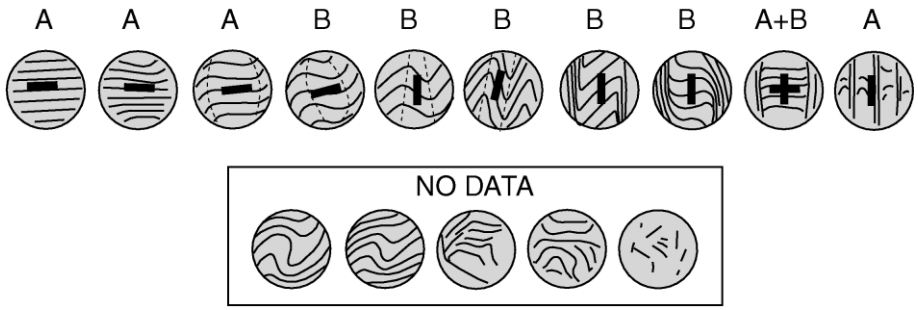

Fig. 3. Schematic sketches of transitional inclusion-trail geometries typically observed in the analysed samples of NW-Iberia. Straight to moderately sigmoidal inclusion trails (A-type data) can be measured directly as indicated with bold bars. They commonly show evidence for having transposed an earlier fabric (extreme right porphyroblast). B-type data correspond to more complex geometries, such as microfolded and/or truncational inclusion trails whose isogons (dashed lines) or truncation surfaces can be measured. Disharmonically folded inclusion trails with strongly curved isogons, or irregular inclusion trail patterns do not yield data. However, their curvature asymmetry (S or Z) can be recorded to apply Bell et al.'s (1995) FIA method.

with subvertical axial planes. The external Cantabrian Zone (CZ) and South-Portuguese Zone (SPZ) show thin-skinned tectonics developed in Upper-Proterozoic to synorogenic Carboniferous Flysch- and Molasse-type deposits.

A total of 28 samples from the 'Basal Unit' (Martínez Catalán et al., 1996) of the allochthonous nappe complex, the underlying para-autochthonous nappe, and the CIZ were analysed with FitPitch (Fig. 2). Samples from the allochthonous and para-autochthonous units are all albite–garnet schists, except one staurolite–andalusite schist. Inclusion trail compositions in some albite–garnet schist samples witness early high-pressure, medium-temperature conditions, followed by a generalised retrogradation of the matrix (Arenas et al., 1995). All CIZ samples are Lower-Palaeozoic micaschists containing andalusite, staurolite, and/or cordierite porphyroblasts.

4.2. Measuring procedure

Radial sets of vertical thin-sections plus one or two horizontal sections were cut from all samples. The angles between all relatively straight inclusion trails in these sections and the thin-section edge were measured and converted to true pitch (vertical sections) or strike angles (horizontal sections). Thin-sections were systematically surveyed by moving them in parallel bands under the microscope and measuring inclusion trails in every new porphyroblast that appeared in the field of view. Measuring orientations for inclusion-trails that are not perfectly straight can be ambiguous and requires strict criteria (Hayward, 1992; Aerden, 1995; Paterson and Vernon, 2001). In the present study, two different types of data were distinguished: (1) orientations of straight to moderately sigmoidal inclusion trails, and (2) orientations for more complexly curved and/or microfolded inclusion trails with relatively straight isogons and/or truncation surfaces. Both types of data will be further referred to as 'A-type' and 'B-type'. Fig. 3 shows the typical inclusion-trail geometries encountered in the samples and illustrates how these were measured. Very smoothly curving or disharmonically folded inclusion trails lacking straight segments were ignored,

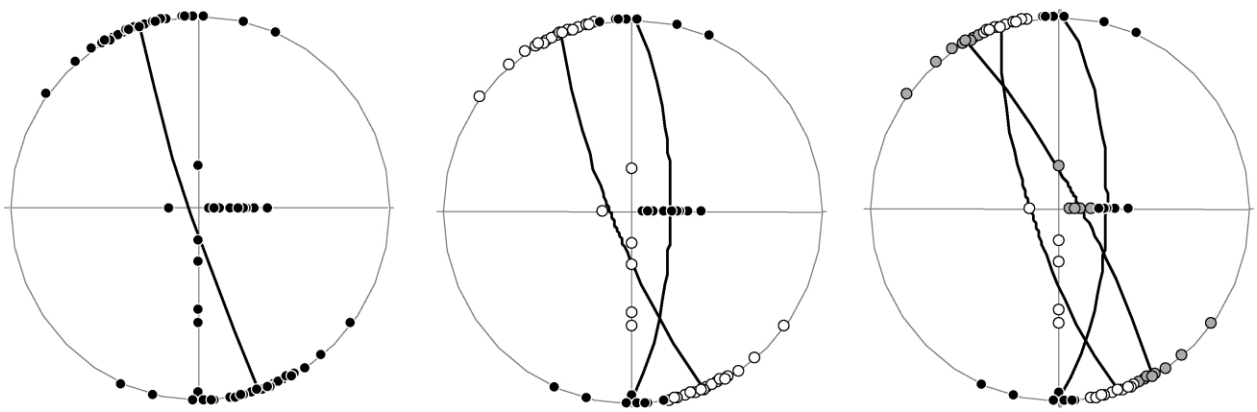

Fig. 4. A-type data for sample 21 (see Fig. 2 for location) fitted to one plane, two planes and three planes. Dots represent inclusion trail orientations measured in three mutually orthogonal thin-sections. Data from individual sections are presented in moving-average rose diagrams (20° counting interval) with the number of data indicated below. A three-plane solution is quantitatively favoured (see Table 1) but is considered an artefact as explained in the text.

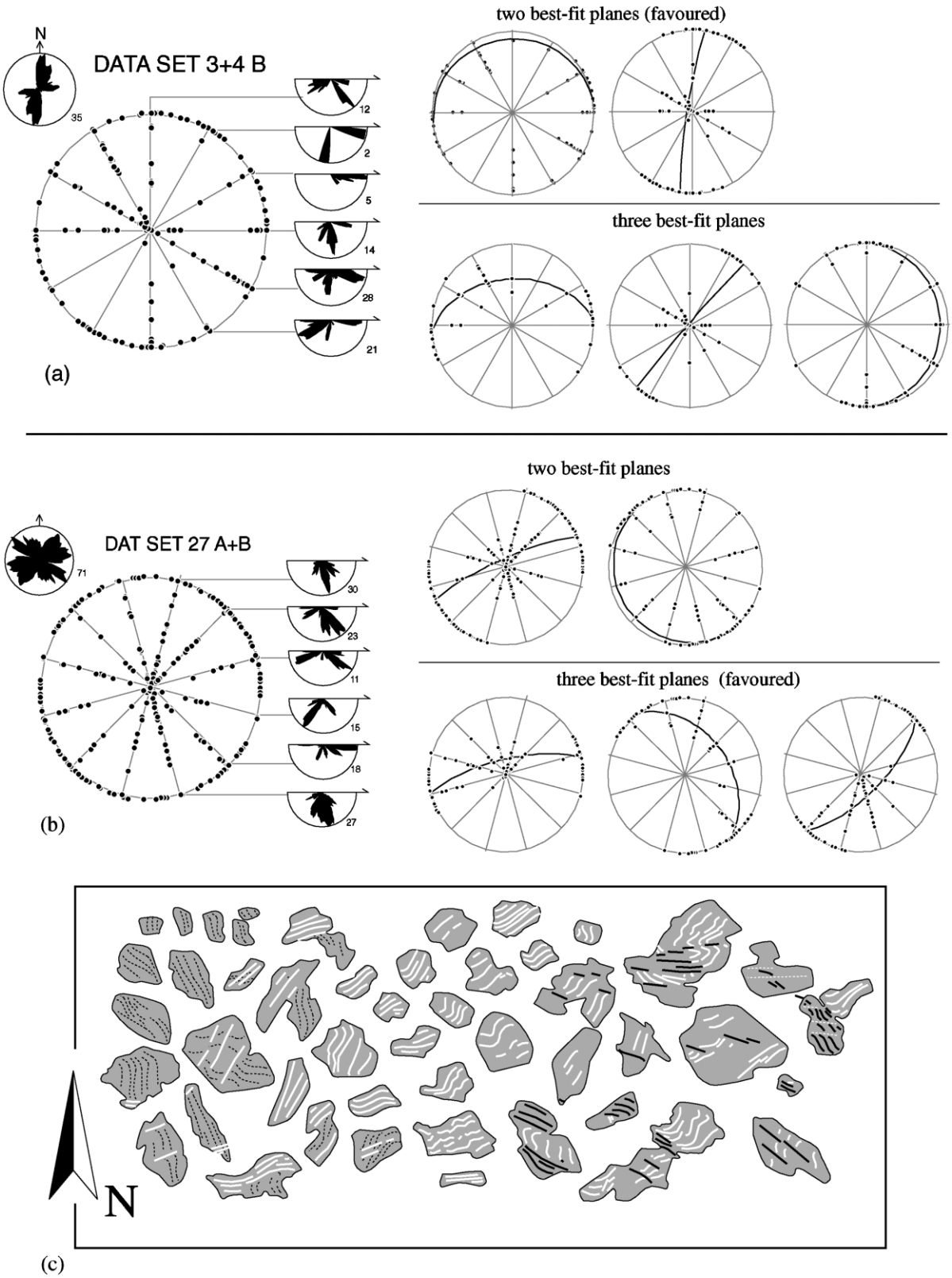

Fig. 5. (a) B-type inclusion trail data from samples 3 and 4 combined (Fig. 2 for sample location) plotted on an equal-area stereonet with accompanying moving average rose diagrams (20° counting sweep) for a total of seven thin-sections used. The smaller stereograms show best-fit solutions with two and three planes. A two-plane fit is favoured as explained in the text. (b) A-type plus B-type inclusion trail data from sample 27 (see Fig. 2b for location) and best-fit solutions with two and three planes. A three-plane fit is favoured as explained in the text. (c) Oriented line drawings of all porphyroblasts observed in a horizontal thin-section of sample 27 showing three fabric generations associated with distinctive trends. These roughly match the strikes of best-fit planes.

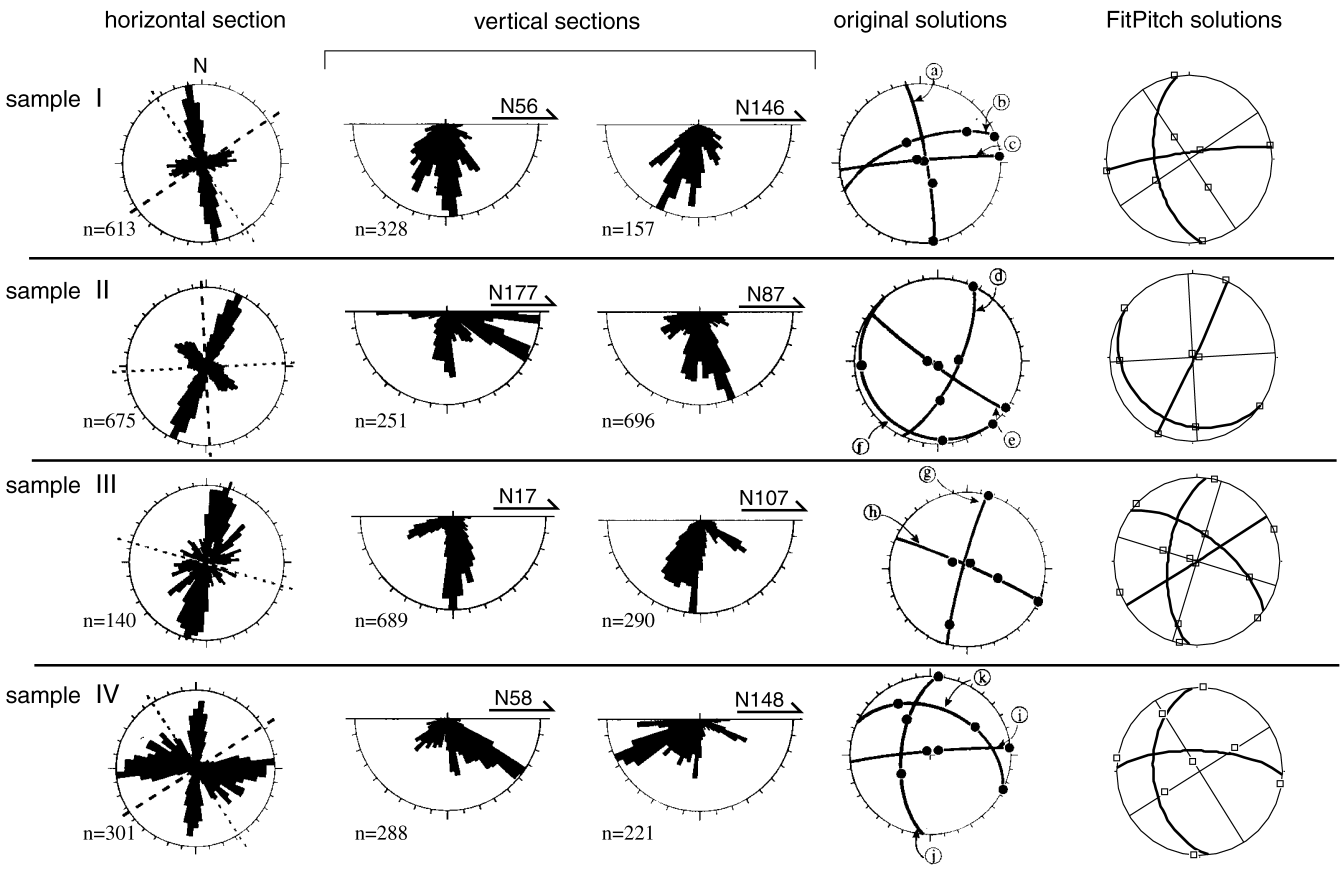

Fig. 6. Microfracture data from samples I–IV of Dezayes et al. (2000; fig. 9) plotted in rose diagrams (5° class intervals and scaled to the same size) and corresponding best-fit solutions as originally proposed and established with FitPitch. The original workers plotted the more prominent modal orientation maxima of the rose diagrams on a stereonet (black dots) and drew several best-fit great circles for them. The FitPitch planes minimise the total deviation of the corresponding intersection lines from individual data. The open square symbols represent best-fit lines as calculated for data from individual thin-sections separately.

as counted for poorly oriented or irregular inclusion trails. Nevertheless, a very large majority of porphyroblasts yielded useful data.

4.3. Results

Due to space limitations, data and best-fit results will only be described for three selected samples in this paper to illustrate the functioning of the program. Data and results for the complete sample set are given as an electronic supplement that can be accessed on the journals home page (http://www.elsevier.com/locate/jsgi), and will be discussed in a separate article (Aerden, 2002, in review).

The first data set considered here corresponds to A-type microstructures in a staurolite–andalusite schist sample of the Basal Unit of the Morais klippen (sample 21; Fig. 2). Inclusion trails in this sample are straight and continuous with, but slightly oblique to, the matrix foliation. They show very constant pitch on a horizontal section and on an E–W-trending vertical section, but more scattered orientations on a third N–S-trending section (Fig. 4). The latter is due to a small angle between this section and the inclusion planes, so that slight variation in foliation orientation is strongly amplified in intersection-line orientation. The single-plane solution for this sample illustrates how the FitPitch program reaches a solution, not by minimising the deviation of data from the model-planes themselves, but from the intersection-lines of those planes. In the opposite case, a plane would have been found passing much closer through the orientation maximum of the E–W section, but highly inconsistent with the pitch angles measured from the N–S section. Judging from R_d and R_m values (Table 1), a three-plane solution is favoured for the sample. However, this is thought to be an artefact caused by slight ‘misfits’ between a limited number of sections available for this sample. Small ‘misfits’ may arise from cumulative errors during reorientation and cutting of samples, but in this case, the origin is sought in gradually changing inclusion trail orientations in a relatively large sample, different parts of which were used for different sections.

The second data set considered here concerns B-type microstructures from two hand specimens combined collected from the same outcrop in the Basal Unit of the Ordenes Complex (samples 3 and 4; Fig. 2). Albite porphyroblasts in the samples exhibit bimodal and suborthogonal inclusion trail orientations corresponding to multiple fabric generations (Fig. 5a; Aerden, 2002). Although R_d is somewhat larger for the three-plane solution than for the two-plane solution, the latter yields a significantly larger R_m value (3.31 versus 2.25) and is therefore considered more adequate.

The third data set presented combines A- and B-type data from an andalusite–staurolite–schist sample of the CIZ (sample 27; Fig. 2). A three-plane solution is favoured in terms of both R_d and R_m (Table 1), and appears in good agreement with the presence of at least three foliation generations with distinctive strikes included in porphyroblasts of different timing (Fig. 5b and c).

5. Application to microfracture data of Dezayes et al. (2000)

Dezayes et al. (2000) studied the orientation of microfractures observed as fluid inclusion trails in quartz grains of a Variscan granite in the Rhine graben. They measured the pitch or strike angles of these fluid-inclusion trails on three mutually orthogonal thin-sections (one horizontal and two vertical) of four borehole samples (samples I to IV). Rose diagrams for these data exhibit roughly bimodal or trimodal distributions reflecting the existence of multiple microfracture sets (fig. 9 of Dezayes et al., 2000; Fig. 6). To find the orientation of these sets, the authors plotted prominent orientation maxima of the rose diagrams on a stereonet and fitted these to two or three great circles. They also measured the orientation of mesoscopic fractures in the vicinity of each sample location (their fig. 10) for comparison with the best-fit planes based on the microscopic data.

Dezayes and coworkers kindly allowed me to analyse their raw data with the FitPitch program to compare its solutions with the best-fit planes established by them. In general terms, our results are in good agreement, although some planes identified originally were not found numerically and vice versa. For sample I, Dezayes et al. (2000) deduced three best-fit planes, whereas FitPitch favours a two-plane solution judging from R_d and R_m values (Fig. 6). Nevertheless, two planes of Dezayes et al. (2000) have very close orientations and are both well approximated by one of the FitPitch planes.

For sample II, a best-fit to two planes is favoured by FitPitch, but three planes were originally identified. The additional plane of Dezayes et al. (2000) (labelled 'e' in Fig. 6) implies that two close orientation maxima with steep but opposite plunges on a vertical E–W-trending section of this sample correlate with two separate strike maxima (NE–SW and NW–SE) on a horizontal section. However, FitPitch correlates these maxima both with the prominent NE–SW strike maximum, while the smaller strike maximum (NW–SE) is linked to a third, more gently plunging maximum on the E–W section. Both FitPitch planes are well matched by two best-fit planes of Dezayes et al. (2000), and by distinctive orientation maxima for mesoscopic fracture planes near the sample location. By contrast, the third plane of Dezayes et al. (2000) (labelled 'e' in Fig. 6) is not witnessed mesoscopically.

Orientations for sample III were fitted to two planes by the original workers, whereas FitPitch slightly favours three planes. Two of these planes roughly match the two planes of Dezayes et al. (2000). The additional third plane (subvertical with ENE–WSW strike) closely matches a prominent orientation maximum for mesoscopic fractures near the sample location (fig. 10c of Dezayes et al., 2000), which suggests it was correctly identified. Finally for sample IV, Dezayes et al. (2000) deduced three best-fit planes, whereas a two-plane solution is favoured by FitPitch. Again, both FitPitch planes are matched by two planes of Dezayes et al. (2000) and by corresponding orientation maxima for mesoscopic fractures (their fig. 10d). However, the third plane of the original workers (labelled 'k' in Fig. 6) is not represented in the mesoscopic fracture data.

6. Discussion

A best-fit solution can always be calculated for any set of data but is not necessarily a meaningful result. If the degree of preferred orientation is very low in a sample or the number of data very limited, then FitPitch may generate meaningless or false solutions. Consequently, solutions must be regarded as statistical approximations to reality, which need to be contrasted with qualitative microstructural observations, and rose diagrams showing the raw data. If a solution appears reasonable, then the significance of best-fit planes must still be interpreted. In the case of inclusion trail data, for example, the number of best-fit planes does not necessarily match the number of foliations included by porphyroblasts. Two best-fit planes may correspond to a single foliation with a bimodal orientation in porphyroblasts, or a single best-fit plane may represent multiple foliation generations with similar orientation.

Concerning the microfracture data of Dezayes et al. (2000), some best-fit planes identified via FitPitch were not recognised by these workers and vice versa, but a majority of planes showed good correspondence. It is remarkable that the additional plane identified by FitPitch (sample III) is well matched by mesoscopic fracture orientations, whereas the contrary is observed for the two extra planes of Dezayes et al. (2000). This does not necessarily imply that the additional planes of Dezayes et al. (2000) are false, but it does perhaps provide impetus for further verification. In any

case, it has been shown that correlating the multimodal orientation maxima between different sections can be ambiguous and in that respect, numerical fitting has the advantage of yielding quantifiable and reproducible results based on every single datum rather than on selected modal maxima.

Concerning porphyroblast analysis, the method has the advantage of being relatively simple and objective only requiring the recognition of three fundamental types of inclusion trail geometries (straight, microfolded, or truncational) without a need to interpret or correlate these. Consequently, samples with relatively poor-quality inclusion trails can still yield useful information. As one is viewing only one or a few porphyroblasts at a time during collection of data, preferred orientation in a thin-section is generally not perceived until data have been converted to true pitch or strike and have been plotted. Even more difficult is anticipating how 2-D orientations measured from different sections will eventually combine in 3-D, which practically excludes biased collection of data.

Porphyroblastic samples that mainly contain very smoothly curving inclusion trails (lacking straight line segments) are not suitable for analysis with FitPitch, but are ideal for the conventional FIA method (see earlier). Conversely, the latter method is not useful for samples that mainly contain straight or inconsistently curving inclusion trails while lacking core-rim curvature reversals. Thus, both methods complement each other. Specific advantages of FitPitch are the possibility to quantify orientational variation of foliations and FIA in a porphyroblast group, and fact that probably fewer thin-sections are required to determine FIA with a comparable resolution. The advantages of the conventional FIA method are its high accuracy (provided a large number of sections are available), and the direct establishment of age relationships between multiple FIA in single samples.

A final point worth mentioning is the non-cylindrical nature of some complex porphyroblast microstructures (e.g. Schoneveld, 1979; Hayward, 1992; Johnson, 1993), which implies that pitch angles of such microstructures will depend on the precise location of the intersecting thin-section plane. However, provided a large enough number of measurements can be made from a thin-section, such variation can be expected to statistically cancel out. In other words, different thin-sections with the same orientation will normally yield similar data sets.

7. Conclusions

The FitPitch computer program is useful for determining the spatial preferred orientation of planar microstructures whose intersection-lines can be measured on different thin-section planes. Examples have been shown of relict foliations in porphyroblasts observed as inclusion trails in thin-section, and microfractures observed as fluid inclusion trails. The program calculates one, two or three best-fit planes by minimising the deviation between measured (microstructural) intersection-lines and hypothetical intersection-lines of a large number of model-planes or model-plane combinations. The degree of fit is quantified by comparing the deviation of real data with the deviation of hypothetical uniform data from the best model intersection-lines. Advantages over qualitative (i.e. visual) fitting of data using a stereonet are that subjective correlation of multimodal orientation maxima between different sections is eliminated, and that solutions are based on every single datum rather than on selected modal maxima. The method complements current techniques for determining FIA orientations for groups of porphyroblasts by allowing calculation of best-fit FIA from a larger range of inclusion-trail types.

Acknowledgements

José-Ramón Martínez Catalán is thanked for discussions that instigated this study. Scott Johnson, Kyuichi Kanagawa and Jürgen Kraus provided very helpful referee reports. With the insights of Richard Lisle they allowed substantial improvement of the original manuscript and widened the scope. Chrystel Dezayes and coworkers are cordially thanked for permitting access to their data and enabling me to test an additional application (microfractures). Thanks to Neil Mancktelow for use of "Stereoplot" and Javier Sanchez San Roman for help with programming. This study was funded by research grants from the Spanish "Dirección General de Investigación Científica y Técnica" coordinated by José-Ramón Martínez Catalán and Francisco Gonzalez Lodeiro.

Appendix A

There is an algorithm that calculates, for every combination of three planes that can be made with the initial 43 model-planes of STEP-1 (Fig. 1a), the sum of deviations between measured (microstructural) intersection-lines and the nearest of three theoretical intersection-lines on the corresponding section. These values (total deviation) are stored in a three-dimensional matrix called SCORE3(i,j,k), where i, j and k identify a particular plane combination. The lowest value in this matrix is localised and the corresponding plane combination identified as the preliminary best-fit solution.

```
                do 160, i=1, 41
                       do 170, j=i+1, 42
                              do 180, k=j+1, 43
                                     do 190, l=1, NUMSEC
                                            do 200, m=COUNTER+1, COUNTER+DATINSEC(l)
                                                   A=abs(MODELPITCH(i,l)-PITCH(m))
                                                   if (A>90) then
                                                          A=abs(180-A)
                                                   end if
                                                   B=abs(MODELPITCH(j,l)-PITCH(m))
                                                   if (B>90) then
                                                          B=abs(180-B)
                                                   end if
                                                   C=abs(MODELPITCH(k,l)-PITCH(m))
                                                   if (C>90) then
                                                          C=abs(180-C)
                                                   end if
                              SCORE3(i,j,k)=SCORE3(i,j,k)+min(A,B,C)/DATINSEC(l)
200                                         continue
                                            COUNTER=COUNTER+DATINSEC(l)
190                                  continue
                                            COUNTER = 0
180                           continue
170                    continue
160             continue
```

KEY:

```
i,j,k : labels of three (out of 43) model planes forming the combination being tested.
NUMSEC : the total number of thin sections
COUNTER : counts the number of loops that have been executed
MODELPITCH (i,l) : model pitch produced by the intersection of model plane "i" with thin section
   "l".
PITCH(m) : value of the "m"th pitch data in section "l"
DATINSEC(l) : the number of data gathered in section "l"
SCORE3(i,j,k) : the sum of angular deviations of measured pitches from model pitches for plane
   combination i,j,k.
```

References

Aerden, D.G.A.M., 1994. Kinematics of orogenic collapse in the Variscan Pyrenees deduced from microstructures in porphyroblastic rocks from the Lys–Caillaouas Massif. Tectonophysics 236, 139–160.

Aerden, D.G.A.M., 1995. Porphyroblast non-rotation during crustal extension in the Variscan Pyrenees. Journal of Structural Geology 17, 709–726.

Aerden, D.G.A.M., 1998. Tectonic evolution of the Montagne Noire and a possible orogenic model for syn-collisional exhumation of deep rocks, Hercynian belt, France. Tectonics 17, 62–79.

Aerden, D.G.A.M., 2002. Correlating deformation in the Iberian Massif (Variscan belt) using relictual fold trends in porphyroblasts and implications for the Ibero-Armorican Arc. Journal of Structural Geology, in review.

Aerden, D.G.A.M., Sanchez San Roman, J., 2002. STEREOFIT: a program for fitting directional data to multiple planes and some applications in structural geology. Computers and Geosciences 28, 81–85.

Arenas, R., Rubio Pascual, F., Díaz García, F., Martínez Catalán, J.R., 1995. High-pressure micro-inclusions and development of an inverted metamorphic gradient in the Santiago Schists (Ordenes Complex, NW Iberian Massif, Spain): evidence of subduction and syncollisional decompression. Journal of Metamorphic Geology 13, 141–164.

Bell, T.H., Mares, V., 1999. Correlating deformation and metamorphism around orogenic arcs. American Mineralogist 84, 1727–1740.

Bell, T.H., Forde, A., Wang, J., 1995. A new indicator of movement direction during orogenesis: measurement technique and application to the Alps. Terra Nova 7, 500–508.

Bell, T.H., Hickey, K.A., Wang, J., 1997. Spiral and staircase inclusion trail axes within garnet and staurolite porphyroblasts from schists of the Bolton Syncline, Connecticut; timing of porphyroblast growth and the effects of fold development. Journal of Metamorphic Geology 15, 467–478.

Bell, T.H., Hickey, K.A., Upton, G.J.G., 1998. Distinguishing and correlating multiple phases of metamorphism across a multiply deformed region using the axes of spiral, staircase, and sigmoidally curved inclusion trails in garnet. Journal of Metamorphic Geology 16, 767–794.

Davis, B.K., 1993. Mechanism of emplacement of the Cannibal Creek Granite with special reference to timing and deformation history of the aureole. Tectonophysics 224, 337–362.

Denison, C., Carlson, W.D., Ketcham, R.A., 1997. Three-dimensional quantitative textural analysis of metamorphic rocks using high-resolution computed X-ray tomography. Part I. Methods and techniques. Journal of Metamorphic Geology 15, 29–44.

Dezayes, C., Villemin, T., Pêcher, A., 2000. Microfracture pattern compared to core-scale fractures in the borehole of Soultz-sous-Forêts granite, Rhine graben, France. Journal of Structural Geology 22, 723–733.

Fyson, W.K., 1980. Fold fabrics and emplacement of an Archean granitoid pluton, Cleft Lake–Gordon Lake area, Slave Province, Northwest Territories. Canadian Journal of Earth Sciences 12, 765–776.

Guglielmo, G. Jr, 1994. Interference between pluton expansion and coaxial tectonic deformation: three-dimensional computer model and field implications. Journal of Structural Geology 16, 237–252.

Hayward, N., 1990. Determination of early fold axis orientations within

multiply deformed rocks using porphyroblasts. Tectonophysics 179, 353–369.

Hayward, N., 1992. Microstructural analysis of the classical spiral garnet porphyroblasts of south-east Vermont: evidence for non-rotation. Journal of Metamorphic Geology 10, 567–587.

Hickey, K.A., Bell, T.H., 1999. Behaviour of rigid objects during deformation and metamorphism: a test using schists from the Bolton syncline, Connecticut, USA. Journal of Metamorphic Geology 17, 211–228.

Huang, W., 1993. Multiphase deformation and displacement within a basement complex on a continental margin: the Wudang Complex in the Qinling Orogen, China. Tectonophysics 224, 305–326.

Ilg, B.R., Karlstrom, K.E., 2000. Porphyroblast inclusion trail geometries in the Grand Canyon: evidence for non-rotation and rotation? Journal of Structural Geology 22, 231–244.

Johnson, S.E., 1990. Deformation history of the Otago schists, New Zealand, from progressively developed porphyroblast-matrix microstructures: uplift-collapse orogenesis and its implications. Journal of Structural Geology 12, 727–746.

Johnson, S.E., 1993. Unravelling the spirals; a serial thin-section study and three-dimensional computer-aided reconstruction of spiral-shaped inclusion trails in garnet porphyroblasts. Journal of Metamorphic Geology 11, 621–634.

Johnson, S.E., Moore, R.R., 1996. De-bugging the "millipede" porphyroblast microstructure; a serial thin-section study and 3-D computer animation. Journal of Metamorphic Geology 14, 3–14.

Jung, W.S., Ree, J.H., Park, Y., 1999. Non-rotation of garnet porphyroblasts and 3-D inclusion trail data—an example from the Imjingang Belt, South Korea. Tectonophysics 307, 381–395.

Mares, V.M., 1998. The structural development of the Soldiers Cap Group within a portion of the eastern foldbelt of the Mount Isa inlier: a succession of near-horizontal and near-vertical deformation events and large-scale shearing. Australian Journal of Earth Sciences 45, 373–388.

Martínez Catalán, J.R., Arenas, R., Díaz García, F., Rubio Pascual, F.J., Abati, J., Marquínez, J., 1996. Variscan exhumation of a subducted Palaeozoic continental margin: the basal units of the Ordenes Complex, Galicia, NW Spain. Tectonics 15, 106–121.

Paterson, S.R., Vernon, R.H., 2001. Inclusion trail patterns in porphyroblasts from the Foothills Terrane, California: a record of orogenesis or local strain heterogeneity? Journal of Metamorphic Geology 19, 351–372.

Ramsay, J.G., 1967. Folding and Fracturing of Rocks, McGraw-Hill, New York, 568pp.

Ries, A.C., Shackleton, R.M., 1971. Catazonal complexes of North-West Spain and North Portugal, remnants of a Hercynian Thrust Plate. Nature 234 (47), 65–79.

Schoneveld, C., 1979. The geometry and significance of inclusion patterns in syntectonic porphyroblasts. Ph.D. Thesis, Institute of Earth Sciences, Utrecht, The Netherlands. 125pp.

Stallard, A., Hickey, K., 2001. Fold mechanisms in the Canton Schist: constraints on the contribution of flexural flow. Journal of Structural Geology 23, 1865–1881.